Influence of Radiation Absorption by Environmental Water Vapor on Radiation Transfer in Wildland Fires

David Frankman[1], Brent W. Webb[1], and Bret W. Butler[2]

Abstract—*Thermal radiation emission from a simulated black flame surface to a fuel bed is analyzed by a ray-tracing technique, tracking emission from points along the flame to locations along the fuel bed while accounting for absorption by environmental water vapor in the intervening medium. The Spectral Line Weighted-sum-of-gray-gases approach was adopted for treating the spectral nature of the radiation. The flame and fuel bed for the simulations are modeled two-dimensionally with the flame being one-tenth as long as the fuel bed. Flame heights of 1 and 10 m were explored, and the angle between the flame and the fuel bed was specified to be either 60 or 90 degrees. Simulated flame temperatures of 1000 K and 1500 K were investigated. The study reveals that water vapor at 100 percent humidity will reduce the incident radiation at the base of a 1000 K flame by 9 percent for a 1 m flame and 16 percent for a 10 m flame oriented normal to the fuel bed. Radiation from an angled flame (oriented at 60 degrees from the fuel bed) experiences slightly less attenuation from water vapor than the 90-degee flame. Further, local attenuation of the hotter flame (1500 K) from environmental water vapor is higher than for the 1000 K flame. The relative effect of the water vapor attenuation is increased with distance from the flame base.*

Introduction

It is understood that thermal radiation transfer plays a significant role in wildland fire spread (De Mestre and others 1989). High temperatures in gaseous and particulate products of combustion result in significant radiation transfer to the unburned fuel ahead of advancing flames. Attenuation of flame radiation can occur from smoke and combustion products that are entrained in the intervening air between flame and fuel. This mechanism for attenuation of flame radiation is a complex function of fuel, flame, wind, and other environmental conditions. It is also recognized that environmental water vapor may be a mechanism for attenuation of flame radiation. However, the magnitude of this influence is unknown. This paper explores the attenuation of radiation from flame to fuel bed by environmental water vapor in the intervening medium.

Literature Review

Wildland fire spread has been modeled using a variety of approaches. Some models attempt to conserve energy generally without separating convection from radiation heat transfer. Still others attempt to model radiation

In: Butler, Bret W.; Cook, Wayne, comps. 2007. The fire environment—innovations, management, and policy; conference proceedings. 26-30 March 2007; Destin, FL. Proceedings RMRS-P-46CD. Fort Collins, CO: U.S. Department of Agriculture, Forest Service, Rocky Mountain Research Station. 662 p. CD-ROM.

[1] Lead author at Department of Mechanical Engineering, Brigham Young University, Provo, UT. dave.frankman@gmail.com

[2] U.S. Department of Agriculture, Forest Service, Rocky Mountain Research Station, Fire Sciences Laboratory, Missoula, MT.

and convection separately (Weber 1991). Those that do model the radiation transfer invoke varied approximations in the radiation submodels. Fons (1946) treats the radiation transfer in an approximate fashion by assuming that a fixed fraction of combustion energy comes from radiation. Emmons (1964) assumes radiation is attenuated with distance from the flame by an exponential relationship. Hottel and others (1965) were the first to model the flame shape, introducing radiation configuration factor relations that quantify the fraction of radiation emitted by one surface that is incident on another. One model considered radiation heat transfer from a planar flame to a planar fuel bed, and the other used a relation that accounted for radiation attenuation through the fuel bed using an exponential factor. Albini (1967) formulated an approach that employed the same radiation sub-model as Hottel and others, considering radiation as the dominant heat transfer mechanism. Thomas (1967) proposed that radiation from the flame was insignificant in comparison to radiation through the porous fuel bed. Other models were introduced using the same radiation configuration factor relations to track radiation transfer from flame to fuel until Cekirge (1978) introduced a formulation that could account for a circular flame front. Albini (1985) first introduced a solution to the Radiative Transfer Equation (RTE), the differential equation governing transport of radiative energy. The RTE was solved using the discrete ordinates method, but no volumetric effects in the fuel, flame, or the intervening medium were included.

To the authors' knowledge, no prior study explores the effect of attenuation of radiation between flame and fuel bed by environmental water vapor. This paper investigates this mechanism for attenuation of flame radiation.

Model

Consider a planar flame of length H and characterized by uniform temperature T_f advancing along a horizontal fuel bed, as shown in figure 1. The length of the fuel bed L is specified arbitrarily in this study to be 10 times the flame length, $L/H = 10$. The angle between flame and fuel bed is ø. Simulations were conducted with and without environmental water vapor in the air separating the flame from the fuel bed. It is assumed that the intervening

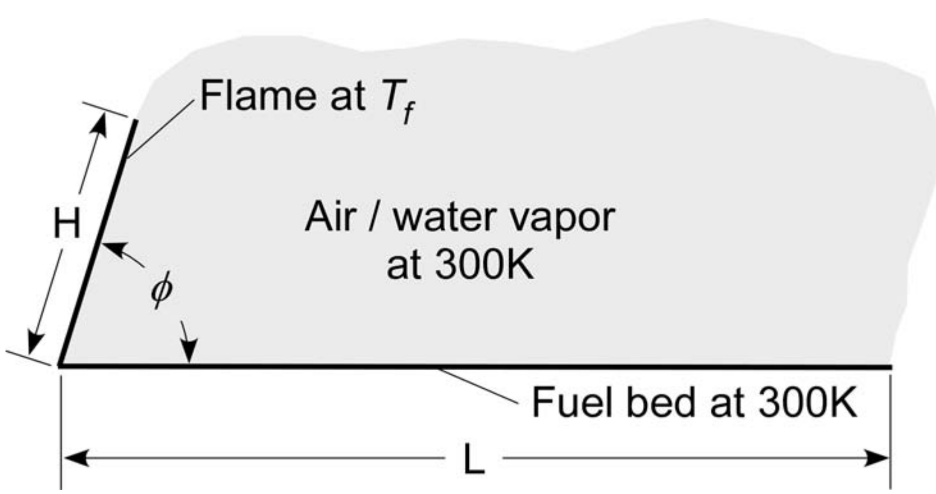

Figure 1 – Schematic illustration of configuration investigated.

medium (air/H_2O vapor) and the fuel bed are at a uniform temperature of 300 K. It should be clearly stated that attenuation by entrained combustion products (ash, H_2O, CO_2, soot, and so forth) is not considered here. Attenuation of flame radiation from such will dominate any effects by environmental water vapor. Rather, the purpose of this study is to characterize solely the effects of water vapor.

Absorption of radiation is governed by the Beer-Lambert Law (Modest 2003), which states

$$I_\eta(s) = I_{\eta o} e^{-\kappa_\eta (s-s_0)} \tag{1}$$

Equation (1) indicates that the spectral radiation intensity of magnitude $I_{\eta o}$ incident on a radiatively absorbing medium and propagating in a particular direction is attenuated exponentially with distance s from the point of incidence s_0 along this direction by the factor $e^{-\kappa_\eta (s-s_o)}$, where κ_η is the volumetric absorption coefficient (Modest 2003). As indicated by the subscript η, equation (1) is a spectral relation; the radiative intensity I_η, incident radiation intensity $I_{\eta o}$, and absorption coefficient κ_η vary with wavenumber (or wavelength). While significant absorption may occur in some regions of the spectrum, others are transparent to radiative transfer. For gases capable of volumetric absorption in the infrared spectrum, the spectral absorption coefficient is characterized by vibration-rotation bands. For water vapor, the principal absorption bands are centered at wavenumbers 3760 and 1600 cm^{-1} (wavelengths of 2.7 and 6.3 μm, respectively). Within each absorption band, thousands of narrow absorption lines exist, with strong absorption of radiation within each narrow line. Several hundred thousand absorption lines are associated with the two principal vibration-rotation bands for water vapor. The absorption strength of each line is a function of the temperature and partial pressure of water vapor. The challenges associated with rigorously modeling mathematically the attenuation of flame radiation by water vapor are significant. The spectral emission characteristics of the flame are a strong function of fuel type, humidity, water content, wind conditions, and so forth. Further, as described herein, absorption of flame radiation by the environmental water vapor occurs within the hundreds of thousands of extremely narrow spectral lines within both infrared vibration-rotation bands. In this study, the flame is characterized as a planar surface whose spectral emission of radiation can be taken to be that of a blackbody at the flame temperature T_f.

The radiative flux from black surface i incident on surface j may be expressed generally as (Modest 2003)

$$q_{i \to j} = \int_0^\infty \int_{A_i} \int_{A_j} e^{-\kappa_\eta s} \frac{\cos\theta_i \cos\theta_j}{\pi s^2} dA_i dA_j E_{bi,\eta} d\eta \tag{2}$$

Equation (2) is a triple integration over wavenumber (η), the area of the emitting surface (A_i), and the incident surface (A_j). The double integration over area is required to track the radiant emission from a location on surface i that arrives at all possible locations on surface j. This tracking must be done for all points of radiation emission on surface i. The geometric term $\cos\theta_i \cos\theta_j / \pi s^2$ accounts for the varying field of view for differential elements on surface i and surface j, separated by a distance s. $E_{bi,\eta}$ is the spectral blackbody emission from surface i, described by the Planck blackbody radiation spectral distribution at the temperature of surface i. The exponential term $e^{-\kappa_\eta s}$ in equation (2) accounts for absorption of radiation by the intervening medium of spectral absorption coefficient κ_η. Integrating over the spectrum as in the development of the classical weighted-sum-of-gray-gases model (Modest 2003), it can be shown that the radiative flux emitted by surface i which is incident on surface j is

$$q_{i\to j} = \int_0^\infty \left(s_i s_j\right)_\eta E_{bi,\eta} d\eta \tag{3}$$

where $\left(s_i s_j\right)_\eta$ is the spectral volumetric exchange factor, expressed as

$$\left(s_i s_j\right)_\eta = \int_{A_i}\int_{A_j} e^{-\kappa_\eta s} \frac{\cos\theta_i \cos\theta_j}{\pi s^2} dA_i dA_j \tag{4}$$

The dependence of both the volumetric exchange factor defined in equation (4), and the total radiant flux, equation (3), on wavenumber is evident. Because of the complex spectral variation in the absorption coefficient of water vapor, the Spectral Line Weighted-sum-of-gray-gases (SLW) model (Denison and Webb 1993a,b) was used to account for its spectral absorption characteristics. The SLW model has been shown to yield accuracy approaching that of computationally intensive line-by-line integrations for a small fraction of the computational cost. Rather than calculate the absorption of flame radiation by integrating on a line-by-line basis over the hundreds of thousands of lines using the Beer-Lambert Law, the SLW model specifies several discrete values of the absorption coefficient κ_k (called gray gas absorption coefficients), determines the total radiation source spectral content corresponding to each discrete value of κ_k (characterized by gray gas weights w_k), and sums (or integrates) the total radiation from a blackbody source over the total number K of discrete gray gas absorption coefficients specified. The integration over a few carefully chosen values of the gray gas absorption coefficient thus takes the place of spectral integration over wavelength in the traditional line-by-line method.

The integration of equation (4) is used to evaluate the radiant flux from one finite area A_i to another A_j. As shown in figure 2, $\varnothing_i$ and $\varnothing_j$ are the angles between the normal vector to each surface and the line joining the differential elements on surfaces i and j, respectively, and s is the distance between the two endpoints of the joining line. In order to determine the variation of local incident flux along the fuel bed, the fuel was divided into small but finite spatial strips running parallel to the shared flame/fuel edge, as shown in figure 2. The incident flux on the fuel was then calculated according to equation (4) for each strip.

Invoking the Spectral Line Weighted-sum-of-gray-gases model, the total (spectrally integrated) radiative flux leaving the planar flame surface and arriving at an arbitrary spatial strip j along the fuel bed may be shown to be the sum of radiative contributions from all gray gases:

$$q_{flame\to fuel,j} = E_{b,flame} \sum_k^K \left(s_{flame} s_{fuel,j}\right)_k w_k \tag{5}$$

where $q_{flame\to fuel,j}$ is the total (spectrally integrated) incident radiation flux emitted by the flame that arrives at (is incident on) strip j along the fuel bed, $E_{b,flame}$ is the total blackbody radiation flux emitted by the flame at temperature T_f, $\left(s_{flame} s_{fuel,j}\right)_k$ is the volumetric exchange factor for radiant transfer from the flame to spatial strip j corresponding to gray gas coefficient κ_k, and w_k is the gray gas weight associated with each gray gas absorption coefficient κ_k. Once the discrete gray gas absorption coefficients κ_k are specified, the corresponding gray gas weights w_k are determined by evaluating the area

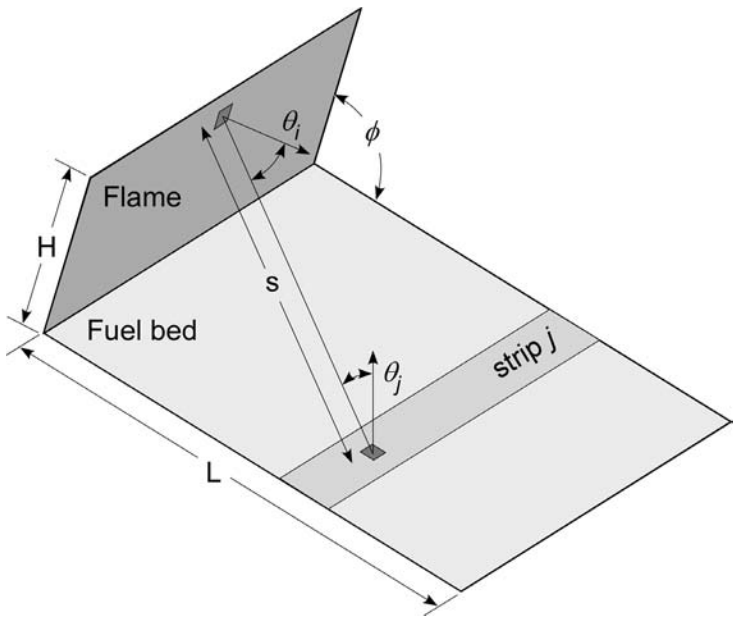

Figure 2—Detailed illustration of geometry and nomenclature for determination of volumetric exchange factor and local incident flux.

under the Planck spectral blackbody radiation distribution $E_{b,flame,\eta}$ where the gray gas absorption coefficient prevails for the gas specie in question (water vapor in this case) (Denison and Webb 1993a). The gray gas weights sum to unity, $\sum_{k}^{K} w_k = 1$. Increasing the number of gray gases employed improves the accuracy of the predictions. In this study, K = 20 gray gases were used in equation (5). Further increases in the number of gray gases yielded no appreciable change in the solution.

Because the closed-form integration of equation (4) to evaluate the volumetric exchange factor for each gray gas, $\left(s_{flame} s_{fuel,j}\right)_k$, is generally not possible for general cases involving radiation attenuation in the intervening medium, the expression was evaluated using numerical integration. Referring again to figure 2, the approach followed here tracks radiation emitted from specified locations along the planar flame to destination strip j along the fuel bed. A reduction of two-dimensional flame and fuel surfaces (shown in fig. 2) to the one-dimensional variation in incident flux along the fuel suggested in figure 1 is not forthcoming in the integration of equation (4). Consequently, two-dimensional flame and fuel bed surfaces were used in the numerical integration as shown. The lateral extent of the flame and fuel surfaces as then sequentially increased in exploratory simulations to determine the dimension large enough to yield the one-dimensional variation in radiative flux along the fuel bed illustrated in figure 1. The lateral dimension required to achieve predictions independent of end effects was 20 times the flame height for all configurations. The surfaces of both flame and fuel were discretized in two directions for numerical evaluation of the integrals in equation (4). The multiple spatial strips along the fuel bed were clustered near the base of the flame in order to accurately resolve the steep gradient of incident radiant flux with position along the fuel. Each strip j was subsequently discretized into smaller differential elements used to evaluate the integrals in equation (4). The numerical integration procedure sweeps through differential area elements on the fuel bed and on each strip of the flame, evaluating the local angles θ_i and θ_j for each of the elements and the corresponding distance s separating the two differential elements in question. The solution thus determines the fraction of radiation emitted by a given element on the flame that is incident on its destination element along the fuel after attenuation by the water vapor in the intervening medium. This accounting must be done for all elements on the flame. The double integration must be performed for the volumetric exchange factor corresponding to each gray gas. Thereafter, the summation over all K gray gases in equation (4) is carried out to determine the total radiative flux.

The volumetric exchange factor $\left(s_{flame}s_{fuel,j}\right)_k$ presented above is identical to the classical configuration factor $F_{i,j}$ (used for predicting radiative exchange between diffuse surfaces in the absence of a radiatively participating intervening medium), with the exception of the exponential absorption term, $e^{-\kappa_k s}$. Analytical expressions for the radiative configuration factor $F_{i,j}$ for commonly encountered surface-to-surface exchange configurations are tabulated in the literature (Siegel and Howell 2002). The accuracy of the evaluation of the volumetric exchange factor can therefore be verified by comparing the numerical integration of equation (4) for the transparent intervening medium case ($\kappa_k \rightarrow 0$) to published analytical expressions for the radiation configuration factor between surfaces with adjoining edges and included angle ø. Figure 3a illustrates the error between the numerically evaluated volumetric exchange factor $\left(s_{flame}s_{fuel,j}\right)_k$ for $\kappa_k \rightarrow 0$ and the corresponding classical radiation configuration factor $F_{i,j}$ (Siegel and Howell 2002) for radiative transport from the entire flame surface to a 10-cm long element at the base of the fuel bed as a function of number of points used in the numerical integration. Both $\phi = 60$ and 90 degree flame configurations for a flame length $H = 1$ m are shown. Radiative exchange between the flame and the small segment at the base was selected for this validation exercise because it is the most rigorous accuracy

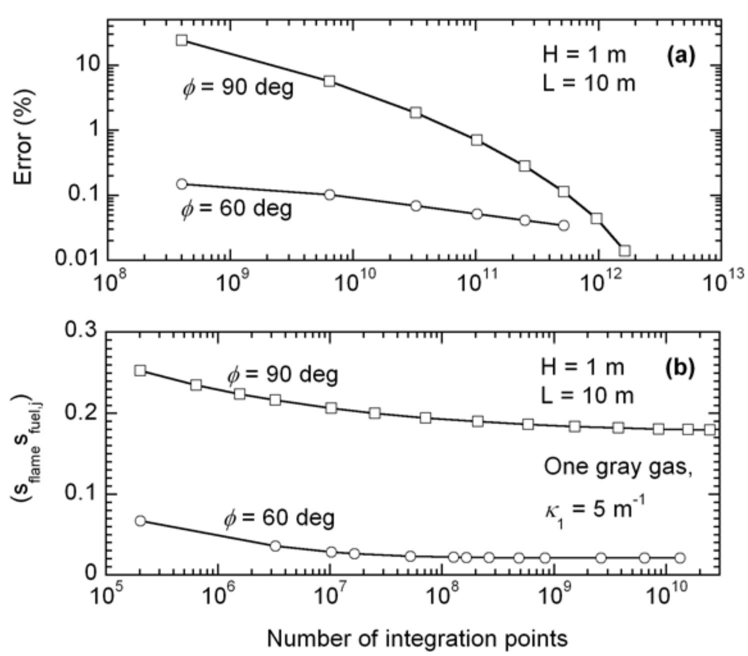

Figure 3—(a) Error between the volumetric exchange factor for $\kappa_k \rightarrow 0$ (for $K = 1$) and the corresponding classical radiation configuration factor, and (b) variation in calculated volumetric exchange factor with number of integration points.

test of the numerical integration. It is for this configuration that the numerical evaluation of the exchange and configuration factors incurs the greatest error. As expected, figure 3a shows that the error decreases as the number of integration points increases. The difference between numerical integration and analytical result is less than 1 percent for a surface discretization employing more than 10^{11} integration points for both flame angle configurations. This favorable comparison for the limiting case $\kappa_k \to 0$ demonstrates the accuracy of the numerical integration of equation (4), if only for the transparent intervening medium case.

While the data of figure 3a constitute evidence that the numerical integration is accurate for the transparent-medium scenario, there is still some uncertainty that with the inclusion of the transmission term $e^{-\kappa_k s}$, the solution may not be convergent. Therefore, a study was undertaken to demonstrate that a convergent solution, independent of the number of points in the numerical integration, was achieved for the case of finite attenuation ($\kappa_k \neq 0$). Figure 3b illustrates the variation in calculated volumetric exchange factor $\left(s_{flame}s_{fuel,j}\right)_k$ between the flame and a fuel bed surface strip near the base of the flame for a single gray gas (K = 1) of gray gas absorption coefficient κ_1 = 5 m^{-1}, with the number of points in the numerical integration for both the normally oriented and angled flame configurations. This value of the gray gas absorption coefficient used in the exercise is in the mid-range of the coefficients used in the simulations reported hereafter in the results. The figure reveals that the value of $\left(s_{flame}s_{fuel,j}\right)_k$ returned by the numerical integration is unchanging beyond 10^{10} integration points for both flame angles studied. Further, to ensure that this choice produced a solution free of round-off error in addition to a solution independent of the number of integration points, all variables associated with the numerical integration were increased in computer precision to confirm that the answer remained the same. It was found that increasing the computer precision (to the so-called "long double" precision) yielded no change in eight significant figures over the double precision results used in all predictions shown hereafter. The results suggest a convergent solution, lending confidence in the accuracy of the volumetric exchange factor for finite gray gas absorption coefficient.

Based on the results of the validation exercise illustrated in figure 3, 10^{11} integration points were used in all simulations reported here. The prediction of incident flux variation along the fuel bed for a given set of conditions was computationally intensive. The calculation of the volumetric exchange factor for each gray gas for all strips on the fuel bed required approximately 12 hours of computation time. This computation was performed for each of the 20 gray gases. In practice, $\left(s_{flame}s_{fuel,j}\right)_k$ was evaluated for all gray gases simultaneously using parallel computing, after which the summation of equation (5) was performed to determine the local radiant flux incident on the fuel.

Results And Discussion

Simulations were conducted for two flame heights, H = 1 and 10 m, with corresponding fuel bed lengths of L = 10 and 100 m, respectively. Included flame angles ϕ of 60 and 90 degrees were explored. Two flame temperatures were investigated, T_f = 1000 and 1500 K, bounding the reasonable nominal range of flame temperatures in wildland fires (Butler and others 2004). All simulations were conducted with and without environmental water vapor in the intervening medium between flame and fuel bed. For those predictions including water vapor, a uniform mole fraction of 3.5 percent H_2O was imposed, corresponding approximately to a relative humidity of 100 percent at a temperature of 300 K. This represents the upper bound on the influence of environmental water vapor on radiation attenuation in wildland fires.

Figure 4 illustrates the variation in predicted local incident radiant flux with position along the fuel bed for a 1 m long flame (H = 1 m) under normal flame conditions (ϕ = 90 deg) for a flame temperature T_f = 1000 K. Two cases are shown, with and without the effect of radiation attenuation by 3.5 percent environmental water vapor. The trends for both cases are qualitatively similar. As expected, the highest flux incident on the fuel bed is at the base

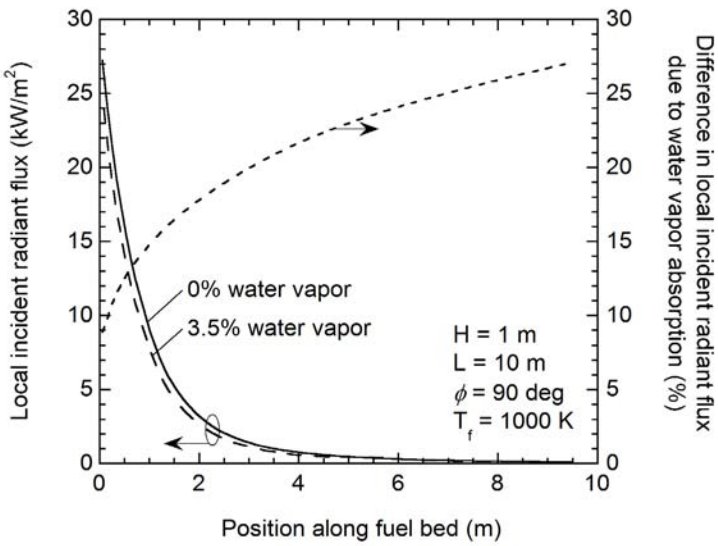

Figure 4—Predicted local incident radiant flux along the fuel bed for the cases with and without water vapor absorption, H = 1 m, L = 10 m, ϕ = 90 deg, and T_f = 1000 K.

of the flame, where the flame is viewed most intensely by the fuel bed. The local radiant flux drops dramatically with increasing distance along the fuel bed. As expected, the influence of water vapor is to attenuate the radiation incident on the fuel bed. At the base of the flame where the radiant flux is the highest, the environmental water vapor reduces the flux incident on the fuel bed by approximately 9 percent. Also plotted in figure 4 is the difference in local incident radiant flux due to water vapor, expressed as a local percentage difference relative to the otherwise identical case with no absorption. The fractional influence of water vapor is lowest near the base of the flame (9 percent), and increases with increasing distance along the fuel bed. This may be explained by the increasing absorbing path length through which emission from the flame must pass for fuel bed locations farther from the flame base. It should be recognized that although the fractional influence is higher farther from the flame, the incident flux decreases rapidly in this direction. Thus, the incident flux is lowest in regions where the percentage influence is highest. The data of figure 4 are used as benchmark against which the parametric effect of varying flame temperature, flame height, and flame angle will be explored in sections to follow.

The effect of varying flame temperature is illustrated in figure 5 for the 1 m, normal flame configuration (ϕ = 90 deg). Predictions for two flame temperatures are presented, T_f = 1000 and 1500 K. As expected, the magnitude of

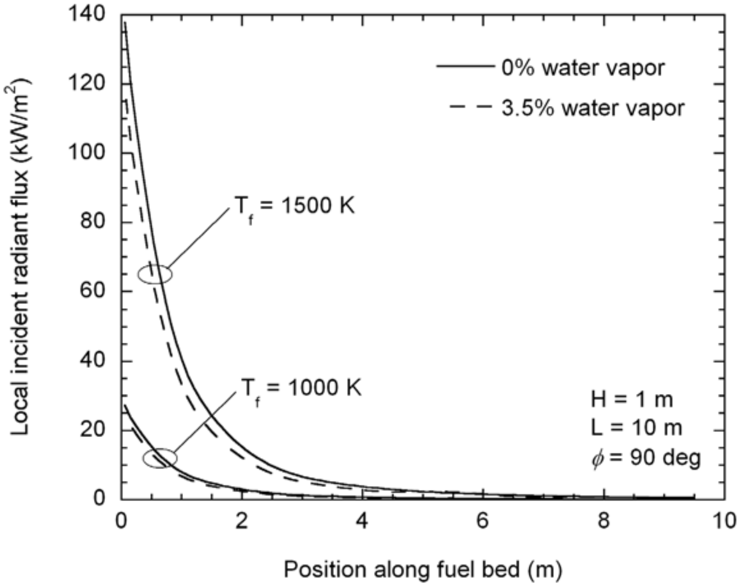

Figure 5—Effect of flame temperature on local incident radiant flux along the fuel bed for H = 1 m, L = 10 m, and ϕ = 90 deg.

the incident flux is considerably higher for the hotter flame. The predictions reveal that the incident radiation at the base of the 1500 K flame is attenuated by water vapor an amount 13 percent relative to the case with no H_2O, compared to 9 percent for the 1000 K flame. The greater influence of water vapor at higher T_f is due to the fact that the spectral emission from the hotter flame is concentrated more heavily in the spectral regions corresponding to the two primary infrared absorption bands of water vapor. It may be concluded that a hotter flame scenario results in greater attenuation by environmental water vapor than is experienced by a relatively cooler flame.

The effect of flame length is shown in figure 6, where local incident flux predictions for H = 1 and 10 m (with L = 10 and 100 m, respectively) are plotted for the normal flame configuration with T_f = 1000 K. The differences

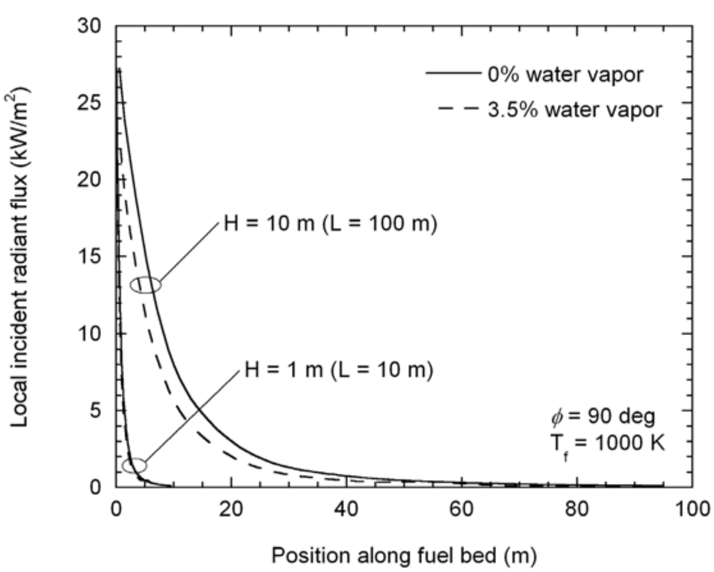

Figure 6—Effect of flame length on local incident radiant flux along the fuel bed for ϕ = 90 deg and T_f = 1000 K.

in flux magnitude near the base of the flame are not significant for the two flame length simulations. This is not surprising, since the region near the flame base "sees" little of the flame beyond the 1 m length, and is therefore exposed to nearly the same radiative environment in both cases. Farther from the flame base along the fuel bed, however, the longer flame yields higher incident flux magnitudes produced by the effect of the additional flame length for H = 10 m. It appears that attenuation of radiation by water vapor is more significant for the longer flame. This may be explained by the fact that radiation from the longer flame must, on average, traverse greater distance of absorbing medium before reaching the fuel bed.

Figure 7 illustrates the influence of flame angle on the incident radiant flux for the 1 m flame, T_f = 1000 K. Relative to the normal flame configuration (ϕ = 90 deg), the radiative flux is substantially higher for the angled flame. As the flame angle decreases from ϕ = 90 degees, it occupies a greater field of view for all locations along the fuel bed. In other words, the fuel bed "sees" the flame more prominently for angled flame conditions, resulting in high incident radiant flux. While not evident in the figure, the fractional decrease in incident flux due to absorption by water vapor is reduced for the angled flame. Whereas the reduction in incident flux at the base of the flame for the ϕ = 90 degee case was 9 percent, the flux is reduced there by only 5 percent for the ϕ = 60 degee case. Again, this may be explained by the fact that the average path length for radiation between flame and fuel bed is smaller for ϕ < 90 degees. Consequently, there is less attenuation by water vapor.

The local influence of flame radiation absorption by water vapor for the cases presented in the foregoing sections is summarized in figure 8. As was done in figure 4, the effect of absorption by water vapor is expressed in figure 8 as a local percentage difference relative to the otherwise identical case with no absorption. To facilitate the presentation of data for both flame lengths studied, the data are plotted as a function of normalized position along the fuel bed, x/L, where x is the coordinate along the fuel bed measured from the base of the flame. For all cases the fractional influence is lowest near the

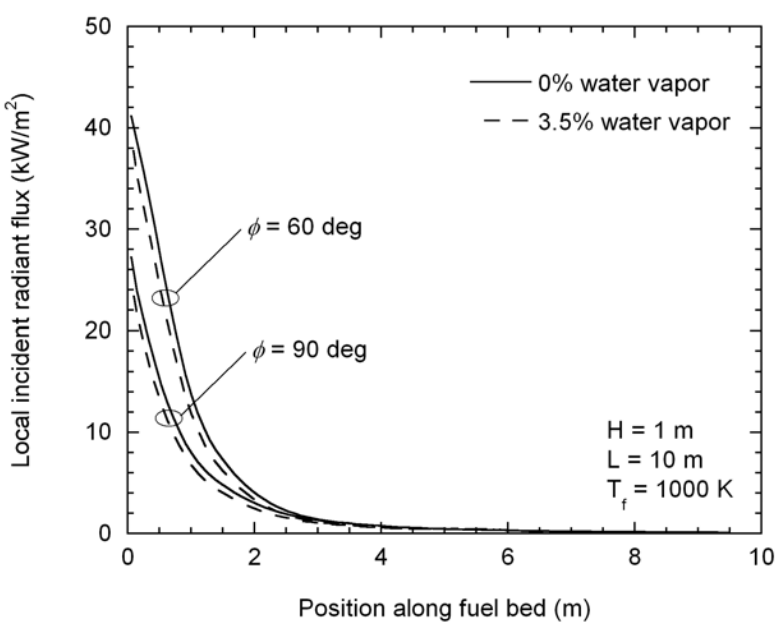

Figure 7—Effect of flame angle on local incident radiant flux along the fuel bed for H = 1 m, L = 10 m, and T_f = 1000 K.

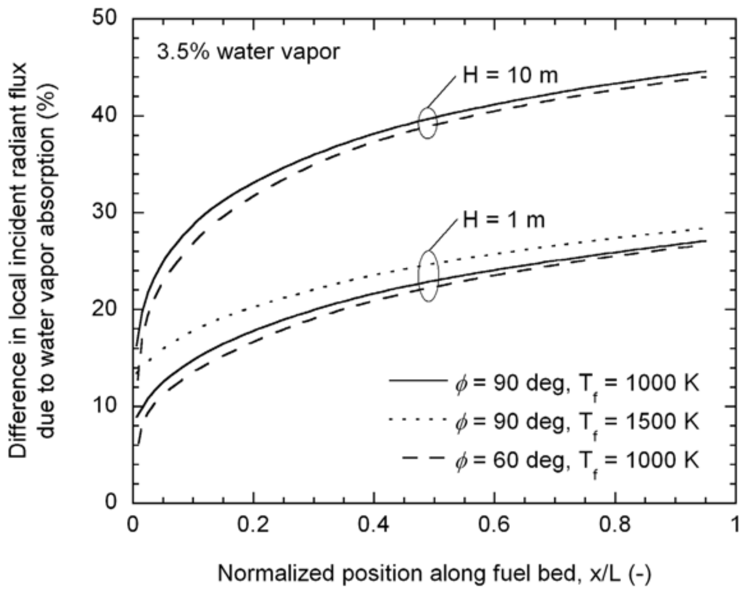

Figure 8—Difference in local incident radiant flux due to water vapor absorption as a function of normalized position along the fuel bed for all cases studied.

base of the flame, and increases with increasing distance along the fuel bed. It should be recognized, however, that although the fractional influence is higher farther from the flame, figures 4 through 7 indicate that the local incident flux decreases rapidly in this direction. Thus, the flux is lowest in regions where the percentage influence is highest. It is again observed that the relative effect of water vapor absorption is greater for increasing flame temperature, flame length, and inclination angle. As outlined previously, this is explained by the greater average path-length through which the flame radiation must pass before arriving at the fuel bed for these scenarios.

The foregoing sections have presented the effect of absorption by environmental water vapor on the *local* radiative flux incident on the fuel bed. Of interest is the aggregate effect of radiation absorption by water vapor on the overall heat transfer to the fuel, found by summing the local incident flux spatially over the entire fuel bed area:

$$Q_{flame\rightarrow fuel} = \sum_j q_{flame\rightarrow fuel,j} A_j \qquad (6)$$

Here, $Q_{flame\rightarrow fuel}$ is the total radiant heat transfer (as opposed to local heat *flux*) emitted by the flame that is incident on the entire fuel bed. The results of the calculation of equation (6) are found in table 1 for all of the cases explored, again expressed as a percentage difference relative to an otherwise identical case with no H_2O absorption. The general trends illustrated by figure 8 are confirmed by the tabulated results. For the range of parameters investigated here, the attenuation of flame radiation by environmental water vapor affects the total heat transfer to the fuel bed by an amount ranging from 11.9 to 26.7 percent. As observed and explained previously, the overall influence of environmental water vapor is less important for lower-temperature flames and for angled flames. While its effect is modest (but perhaps nonnegligible) for small flames, it can become quite significant for larger flames.

Table 1—Overall reduction in total radiative heat transfer incident on the fuel bed due to absorption by environmental water vapor.

Flame length	ϕ = 90 deg T_f = 1000 K	ϕ = 90 deg T_f = 1500 K	ϕ = 60 deg T_f = 1000 K
H = 1 m (L = 10 m):	13.5 percent	16.7 percent	11.9 percent
H = 10 m (L = 100 m):	26.7 percent		25.1 percent

Conclusions

Predictions have been made for radiative transfer from black, isothermal, planar flame to a black fuel bed maintained at 300 K. The effect of flame inclination, flame temperature, and flame length were explored for cases with and without absorption by environmental water vapor in the intervening air (at 300 K). From these simulations one can see that, depending on the conditions, water vapor has a modest but nonnegligible effect on the radiative transfer from flame to fuel. The effect is more pronounced for larger flames at higher flame temperatures. The influence of water vapor on attenuation of radiation is reduced for angled flames.

References

Albini, F.A. 1967. A physical model for fire spread in brush. Pittsburg, PA: Eleventh Symposium (Int.) on Combustion, The Combustion Institute: 533-560.

Albini, F.A. 1985. A model for fire spread in wildland fuels by radiation. Combustion Science and Technology. 22:229-258.

Butler, B.W.; Cohen, J.; Lathan, D.J.; Schuette, R.D.; Sopko, P.; Shannon, K.S.; Jimenez, D.; Bradshaw, L.S. 2004. Measurements of radiant emissive power and temperatures in crown fires. Canadian Journal of Forest Research. 34:1577-1587.

Catchpole, W.R.; Catchpole, E.A.; Tate, A.G.; Butler, B.W.; Rothermel, R.C. 2002. A model for the steady spread of fire through a homogeneous fuel bed. Forest Fire Research and Wildland Fire Safety. Rotterdam: Millpress. ISBN 90-77017-72-0.

Cekirge, H.M. 1978. Propagation of fire fronts in forests. Computers and Mathematical Applications. 4:325-332.

De Mestre, N.J.; Catchpole, E.A.; Anderson, D.H.; Rothermel, R.C. 1989. Uniform propagation of a planar fire front without wind. Combustion Science and Technology. 65: 231-244.

Denison, M.K.; Webb, B.W. 1993a. A spectral line-based weighted-sum-of-gray-gases model for arbitrary RTE solvers. ASME Journal of Heat Transfer. 115:1004-1012.

Denison, M.K.; Webb, B.W. 1993b. An absorption-line blackbody distribution function for efficient calculation of gas radiative transfer. Journal of Quantitative Spectroscopy and Radiative Transfer. 50:499-510.

Emmons, H. 1964. Fire in the forest. Fire Research Abs. Rev. 5:163-178

Fons, W.L. 1946. Analysis of fire spread in light forest fuels. Journal of Agricultural Research. 72:93-121.

Hottel, H.C.; Williams, G.C.; Steward, R.R. 1965. The modeling of firespread through a fuel bed. Tenth Symposium (Int.) on Combustion. Pittsburg, PA: The Combustion Institute: 997-1007.

Modest, M.F. 2003. Radiative Heat Transfer, 2nd Edition. New York: Academic Press.

Siegel, R.; Howell, J.R. 2002. Thermal Radiation Heat Transfer, 4th Edition. New York: Taylor and Francis.

Thomas, P. H. 1967. Some aspects of the growth and spread of fire in the open. Forestry. 40:139-164

Weber, R.O. 1989. Analytical models for fire spread due to radiation. Combustion and Flame. 78:398-408.

Weber, R.O. 1991. Modelling fire spread through fuel beds. Progress in Energy and Combustion Science. 17:67-82.